Nanomed J. 12(2): 226-237, Spring 2025

RESEARCH PAPER

# Synergistic co-administration of doxorubicin and berberine by PLGA/PVA hybrid polymeric Nanoformulation for breast cancer treatment

***Masoumeh Rahmani [1], Mahdieh Hemati [2, 3], Milad Akhlaghi [2], Bibi Fatemeh Haghiralsadat [1, 3]*, Fatemeh Oroojalian [4, 5]****

*[1]Department of Advanced Medical Sciences and Technologies, School of Paramedicine, Shahid Sadoughi University of Medical Sciences, Yazd, Iran*
*[2]Department of Clinical Biochemistry, Faculty of Medicine, Shahid Sadoughi University of Medical Sciences, Yazd, Iran*
*[3]Medical Nanotechnology and Tissue Engineering Research Center, Yazd Reproductive Sciences Institute, Shahid Sadoughi University of Medical Sciences, Yazd, Iran*
*[4]Natural Products and Medicinal Plants Research Center North Khorasan University of Medical Sciences Bojnūrd, Iran*
*[5]Department of Medical Nanotechnology, School of Medicine, North Khorasan University of Medical Sciences, Bojnūrd, Iran*

## ABSTRACT

***Objective(s):*** The clinical application of doxorubicin (DOX), a potent anticancer agent, is restricted by its serious side-effects and multidrug resistance. The combination strategy of antineoplastic drugs with Berberine (BBR) as plant-derived natural products enhances the cytotoxicity of chemotherapeutic drugs in cancer cells and also amends their toxicity in normal cells.

***Materials and Methods:*** In this study, the nanoparticles (NPs) of PLGA/PVA containing DOX and BBR were synthesized and optimized using the double emulsion-solvent evaporation method. The vesicular size, zeta potential, entrapment efficiency and also the drug release profile was surveyed at different temperatures and pH (37 °C, 7.4 and 42 °C, 5.2). The MTT assay was used to evaluate the cytotoxic effects of individual of DOX and BBR as a free form and as a nanoparticle form and also the combination of DOX- and BBR-loaded NPs on MCF-7 breast cancer cells.

***Results:*** The optimum formulation demonstrated that the vesicle size and zeta potential of DOX were 176.4 nm and -56.4 mV and BBR were 150.3 nm and -41.2 mV, respectively. Entrapment efficiency (EE%) for DOX and BBR was 91.0 ± 1.9% and 82.0 ± 1.8%, respectively. The DOX- and BBR -loaded NPs exhibited a sustained and controlled release pattern with the pH- and thermosensitive characteristic. Additionally, the loading of DOX and BBR into PLGA/PVA NPs had a higher toxicity against cancer cells when compared with free forms and the combination of DOX and BBR was exhibited an augmented antineoplastic activity against the cancer cell death.

***Conclusion:*** The findings of this study suggest that the coadministration of DOX with BBR using the PLGA/PVA NPs may have the potential clinical application in sensitization cells to DOX and generates synergistic antitumor effects.

***Keywords:*** *Berberine, Breast cancer, Doxorubicin, PLGA, PVA*

**How to cite this article**
*Rahmani M, Hemati M, Akhlaghi M, Haghiralsadat BF, Oroojalian F. Synergistic co-administration of doxorubicin and berberine by PLGA/PVA hybrid polymeric formulations for breast cancer treatment. Nanomed J. 2025; 12(2): 226-237. DOI: 10.22038/nmj.2024.79160.1945*

## INTRODUCTION

Doxorubicin (DOX) as cytotoxic anthracycline, has been extensively used in treating a wide range of cancers such as lymphomas, leukemia, breast cancer and osteogenic sarcoma [1, 2]. However, congestive heart failure (CHF), acute cardiotoxicity and multidrug resistance are the consequences of long-term administration of DOX [3-5]. Recently, combination chemotherapy of two or more therapeutic agents including

* *Corresponding authors: Emails: fhaghirosadat@gmail.com; f.oroojalian@nkums.ac.ir; Oroojalian.f@gmail.com*
Note. This manuscript was submitted on April 6, 2024; approved on Jun 2, 2024

[1] multiple chemotherapeutic drugs or [2] simultaneous administrating of chemotherapeutic drugs with natural products has been dramatically developed since it could regulate different signaling pathways in cancer cells, reduce adverse side effects and minimize multidrug resistance [6-9]. This phenomenon caused a synergistic response that increases treatment efficacies and reduces dosage of each drug [10]. Berberine (BBR) as a botanical isoquinoline alkaloid exhibits effective pharmacological activities including anticancer, antidiabetic, hypoglycemic, antioxidant, antibacterial, anti-inflammatory, antiatherosclerotic, hepatoprotective, cardioprotective and chemopreventive properties [11-15]. Also, BBR indicates the considerable inhibitory actions against the proliferation of tumor cells. The apoptotic role of BBR is attributed to activation of pro-apoptotic genes of intrinsic apoptotic pathway, caspase-3 and−8 which release cytochrome c. In addition BBR induces reactive oxygen species (ROS) production in cancer cells that lead to triggering apoptosis pathway [16]. As an aside, BBR arrest the cell cycle tumor cells at G1 phase at lower concentrations and G2/M phase of cell cycle at higher concentrations that inhibits cancer cells growth. BBR as herbal medicine not only has been shown to affect cell apoptosis and the tumor microenvironment and inhibits cancer cell proliferation but also has been exhibited the protective effect on normal cells [17]. Therefore, BBR could act as a promising drug candidate for drug formulation with chemotherapy drugs against cancer cells. However, poor stability and low absorption rate impede its clinical bioavailability. Also administration of free dugs reduces significant antitumor effect and enhances normal tissue toxicity. These has led toward the development of a novel drug delivery system to attain local drug accumulation, improve drug bioavailability, extend the half-life of drug and prolong systemic circulation [18-21]. Nanocarriers enhance permeability and retention (EPR) effect and strengthen passive targeting that result in the accumulation of loaded drugs into tumor tissues. In various studies, other types of nanoparticles were used as drug delivery carriers for DOX, such as lipid-based nanoparticles, dendrimer, carbon-nanomaterials, polymeric nanoparticles and etc. This work represents a PLGA/PVA nanoparticle as drug delivery system to transfer DOX and BBR to cancer tissue. Poly (lactic-co-glycolic acid) (PLGA) become popular as the high molecular weight synthetic nanoparticle (NP) owing to non-toxic, modifiable, biodegradable, biocompatible and that can contentiously release various anticancer agents [22]. Polyvinyl alcohol (PVA) is applied to stabilize PLGA nanoparticles and prevent its agglomeration. PLGA/PVA systems can control the drug release with thermo- and pH dual sensitive behavior that lead to keeping constant plasma drug concentration at a certain time, minimizing dosing times and obliterating side effects by targeted antitumor drug release [2, 23-25]. So, the aim of this study is to analyze and optimize the effect of various variables including the amount of PVA, different molar ratio of drug to polymer, type of organic phase on the entrapment efficiency percentage (EE%) of DOX/BBR-loaded PLGA/PVA (DOX-NPs and BBR-NPs) nanoparticles and the release profile. Evaluation the physiochemical properties of the optimal formula, and comparing the cytotoxicity of free form of DOX and BBR to encapsulated form of them on cancerous cell.

## MATERIALS AND METHODS

### *Materials*

Doxorubicin HCl (DOX) was obtained from Ebewe Pharma (Austria). Poly (d,l-lactic-*co*-glycolic acid) (50:50) with molecular weight 11,700 and BBR powder were purchased from Sigma Aldrich Co. (St. Louis, MO, USA). Dichloromethane (DCM) and Polyvinyl alcohol (PVA) were procured from Merck, Germany. Chloroform, dialysis bag, PBS tablets, DMSO (dimethyl sulfoxide) and MTT (3 – (4, 5-dime-thylthiazol-2-yl)-2, 5-diphenyl tetrazolium bromide) were supplied from Sigma-Aldrich (St. Louis, MO).

### *Preparation of PLGA Nanoparticles*

In the double emulsion-solvent evaporation method (W1/O/W2), DOX solution and BBR powder as the stock of the initial aqueous phase (W1) were dissolved in a certain volume of distilled water. Thereafter, 0.01 g of PLGA polymer was dissolved in 1 ml of the organic phase consisting of either chloroform or dichloromethane (DCM) and vortexed until the polymer was completely dissolved. The aqueous phase was then added to the organic phase (W1/O) and sonicated with power of 100 w for 5 min. In the next step, the above solution were emulsified after the addition of 2 mL of varying concentrations of (1% and 4% *w/v*) of polyvinyl alcohol (PVA) as the second aqueous phase by pulse sonication using a probe sonicator on an ice bath for 8 min. Then, the W1/O/W2 emulsion was added to 5 ml of 0.1% PVA under gentle magnetic stirring to evaporate the organic

solvent and complete formation of nanoparticles. Finally, after 16 hours, the suspended PLGA-NPs were centrifuged at 14,000 rpm for 15 min, the supernatant was rinsed off, and the precipitate was purified after washing with deionized water for three times. The obtained NPs were washed to separate the free drugs and then freeze-dried and stored at −20 °C for further experiments. In this study, to optimize nanoparticles based on the entrapment efficiency and release rate, different formulations of PLGA polymer containing DOX (PLGA- DOX) and BBR (PLGA-BBR) were synthesized with different concentration ratio of drug to polymer, type of organic phase, different PVA% and the optimal formulation was selected (Table 1) [14].

***Physicochemical properties of PLGA polymer nanoparticles***

The mean particle size and zeta potential of the developed PLGA-NPs were analyzed by dynamic laser diffraction technique using a ZetaSizer device (Horiba SZ-100, Horiba Mfg. Co. Ltd, Kyoto, Japan). The shape and surface morphology of the PLGA-NPs were imaged and determined by micrographs of the NPs obtained by Field Emission Scanning Electron Microscopy (FESEM) (Zeiss SIGMA, VP) with a diluted sample (0.1 mg/mL) that was coated with a layer of gold. Atomic Force microscopy (Nanowizard □; JPK instruments; Germany) also was used for assessment of NPs' 3D structure and after diluting samples (1:1000) with distilled water, homogenizing was performed by sonication for 30 min and the prepared samples for imaging placed on mica sheets.

***Standard calibration curves and Entrapment efficiency evaluation***

In order to evaluate the DOX and BBR entrapment efficiency and their release profile from nanoparticles, two standard curves with DMSO and PBS (Phosphate Buffered Saline) were plotted, respectively. So, different serial dilution of DOX and BBR was prepared in DMSO/PBS solvent and the adsorption was read at a lambda max wavelength (λmax) of DOX=480 nm and BBR=340 nm by UV/V is spectrophotometer (Epoch, USA) with three repetitions and its standard calibration curves were drawn.

To ascertain the entrapment efficiency of DOX and BBR, nanoparticles were centrifuged (concentration of 1 mg/mL), the supernatant was harvested and its absorbance was read at λmax of DOX=480 nm and BBR= 340 nm. Then, the concentration of supernatant as unloaded drug in nanoparticles was obtained based on the standard calibration curve of DOX and BBR in PBS. The percentage of entrapment efficiency (EE%) was calculated as follows:

EE% = Concentration of total drug - Concentration of unencapsulated drug/ Concentration of total drug × 100

***In vitro thermo- and pH-sensitive DOX and BBR-NPs release assay***

The release of DOX and BBR from PLGA/PVA NPs was monitored using a 12 kDa cut-off dialysis bag against PBS for 72 hr at 37 °C and 42 °C temperatures (For stability assessment) and pH 7.4, 5.2. The samples were placed in a dialysis bag and suspended in the tube containing PBS (pH 7.4, 5.2) on a hitter stirrer (RPM=75). Then at specific time, 500 µL of buffer surrounding dialysis bag was removed and replaced with 500 µL of fresh PBS buffer. The absorbance of samples was read using the UV/Vis spectrophotometer at λmax of each drug and the amount of released DOX/BBR was analyzed using standard curve in PBS [20, 26].

***Viability study***

To measure the cytotoxicity of free DOX

Table 1. Encapsulation efficiency and release rate in different synthesized formulations. *: optimal formula

| Formula | Polymer/Drug | PVA% | Solvent PLGA | Encapsulation Efficiency (%EE) | % Release (72 hr) pH 7.4 and 37 °C | % Release (72 hr) pH 5.2 and 42 °C |
|---|---|---|---|---|---|---|
| F1 | 1/20 | 1% | Chloroform | DOX: 25.0 ± 0.7<br>BBR: 17 ± 1.5 | DOX: 25.6 ± 3.8<br>BBR: 27.0 ± 0.5 | DOX: 20.2 ± 2.5<br>BBR: 30.8 ± 1.5 |
| F2 | 1/20 | 4% | Chloroform | DOX: 27.0 ± 1.6<br>BBR: 31.5 ± 1.2 | DOX 16.3 ± 1.5<br>BBR: 19.6 ± 2.5 | DOX: 29.7 ± 1.9<br>BBR: 25.3 ± 1.9 |
| F3 | 1/20 | 4% | DCM | DOX: 49.0 ± 1.8<br>BBR: 53.0 ± 2.3 | DOX: 46.0 ± 1.4<br>BBR: 38.8 ± 3.6 | DOX: 62.0 ± 1.1<br>BBR: 50.5±1.6 |
| F4 | 1/10 | 1% | DCM | DOX: 70.2 ± 2.7<br>BBR: 68.1 ± 0.25 | DOX: 62.5 ± 2.3<br>BBR: 55.7 ± 2.8 | DOX: 79.0 ± 1.5<br>BBR: 76.5 ± 1.1 |
| F5* | 1/10 | 4% | DCM | DOX: 91.0 ± 1.9<br>BBR: 82 ± 1.8 | DOX: 51.3 ± 2.7<br>BBR: 44.1 ± 1.8 | DOX: 70.0 ± 0.9<br>BBR: 67.9 ± 0.5 |

(15.62, 31.25, 62.5, 125, 250, 500 µg/mL), free BBR (62.5, 125, 250, 500, 750, 1000 µg/mL), DOX -loaded PLGA, BBR-loaded PLGA, blank PLGA and combination DOX and BBR PLGA, MTT assay was carried out. MCF-10A as a model for normal human mammary epithelial cells and MCF-7 cell line as a breast cancer cell, were purchased from the Pasture instituted of Iran. Briefly, $10^4$ cells were cultured in 96 well plates. After 24 hr, the cells were incubated with the above mentioned formulation in the absence of the serum for 48h. Then, the contents of each well were withdrawn and incubated with 20 µL of MTT solution (0.5 mg/ml) for 4 hr. The resultant formazan crystals were dissolved in DMSO and the intensity of coloration of obtained samples was measured using EPOCH microplate spectrophotometer (synergy HTX, Bio-Tek, Winooski, VT) at 570 nm [14, 26-29].

***Statistical analysis***

The examination were performed in triplicate (n= 3) and the results were represented as mean with standard deviation (mean ± SD). Data were analyzed and compared by the student t-test and ANOVA using GraphPad Prism 8 (GraphPad, San Diego, CA). The P-value < 0.05) was considered as statistically significant.

## RESULTS AND DISCUSSION

***Optimization of DOX-PLGA NPs and BBR-PLGA NPs Characteristics***

To prepare NPs with high encapsulation efficiency and desired release rate, various parameters including PVA amount, solvent type (chloroform/dichloromethane) and the molar ratio of polymer/drug were optimized. As shown in Table 1, the optimum results in terms of the highest entrapment of DOX and BBR (91.0 ± 1.9 % and 82.0 ± 1.8 %) and the optimum cumulative release of DOX and BBR (70.0 ± 0.9 % and 67.9 ± 0.5 %) at 42 °C and pH 5.2 for 72 hr were achieved when dichloromethane as organic phase and 4% solution of PVA as an emulsifier with the molar ratio of polymer/drug =10 was used. The application of DCM instead of chloroform (F2 vs F3) as an organic solvent provided a good encapsulation of DOX and BBR but the release rate of the NPs prepared by using chloroform were more confined than that of the NPs prepared by using DCM [30]. F4 and F5 were composed of 1% and 4% PVA, respectively. According to the results, the PLGA formula containing 4% PVA showed higher drug entrapment compared to F4. However, the percentage of drug release was higher for F4 compared to F5. Alshamsan et al. prepared PLGA-loaded indomethacin by the single-emulsion solvent evaporation technique using dichloromethane (DCM)/chloroform with Polyvinyl-alcohol (PVA)/ Polyvinylpyrrolidone (PVP) and investigated the effects of different proportions of PVA with DCM/ chloroform on the physiochemical properties, entrapment efficiency and release amount. They declared the highest encapsulation and appropriate release was found with PLGA-NPs made of 3% PVA and DCM compared to 1% PVA and chloroform that was consistent with our results [31]. Fuminori et al. prepared the hydrophilic-drug-containing PLGA microspheres with chloroform or DCM and studied the release profile of the PLGA microspheres using DCM or chloroform. They represented that the release rate of the microspheres fabricated by DCM were higher than that of the microspheres fabricated by chloroform. It is attributed to the distributed location of hydrophilic-drug at the center or core of the NPs prepared by using chloroform that result in the delayed initial release into the water phase [30]. Accordingly, in the present study, we investigated the ratios of 1/20 and 1/10 in development of nanoparticles (F3 vs F4) (To clarify, the ratios mentioned refer to the drug-to-polymer ratio. Thus, a ratio of 1/10 indicates there is one part of drug to ten parts of polymer, and similarly, a ratio of 1/20 indicates one part of drug to twenty parts of polymer.). The findings showed that by increasing the ratio of drug to polymer, the entrapment efficiency of DOX and BBR nanoparticles was increased from 49% to 70.2% and 53% to 68.1%, respectively. These results are in line with other studies [14]. F5 was selected as the optimal formula and used for further studies and analysis. The molecular weight of the optimal formula was 20 K Dalton.

***Physicochemical properties of PLGA NPs***

Based on the results acquired from Zeta Sizer, the average size of DOX and BBR polymer nanoparticles was 176.4 and 150.3 nm, PDI was 0.769 and 0.285 and their zeta potential was -56.4 and -41.2 mV, respectively (Table 2). These nano-sized particles overcome biological barriers and increase DOX and BBR accumulation in

Table 2. The size, zeta potential and PDI of DOX-NPs and BBR-NPs

| | Size (nm) | Zeta Potential (mV) | PDI |
|---|---|---|---|
| DOX-NPs | 176.4 | -56.4 | 0.769 |
| BBR-NPs | 150.3 | -41.2 | 0.285 |

target tissue by the enhanced permeability and retention effect (EPR) and prolong the circulation time in blood [32]. Large negative or positive of zeta potential prevent the degree of nanoparticles agglomeration by high electrostatic repulsion and increase their physical stability in an aqueous medium [14, 33]. Also negative zeta potential inhibits the interactions between nanoparticles and blood components and stimulation of the immune system [34]. Hendriks et al. investigated the effect of NP properties such as zeta potential on its cellular internalization. They demonstrated that increasing surface charges, either positive or negative, have been displayed to enhance particle uptake in comparison with uncharged NPs [35]. Zhang et al synthesized three formulations with negatively, weakly positively and strongly positively charge to understand the effect of surface charge on the cellular uptake. It is found that the surface charge for nano-sized particles play an important role on the cellular internalization process and the higher zeta potential and larger the surface-to-volume ratio of the nanoparticles increase the more cellular uptake of nanoparticles [36]. The FESEM images of the PLGA nanocapsules developed under optimum conditions indicate the smooth surface, a near- spherical shape, and the average size of about 150 nm. The particle size was further confirmed by FESEM image, which was in good coordination with the DLS result. The photographs obtained by AFM (Nanowizard®, JPK) techniques also show that the NPs have appropriate 3D structures which are in accordance to the data of FESEM and DLS analysis.

### *Drug release behavior of PLGA NPs*

In order to calculate the amount of DOX and

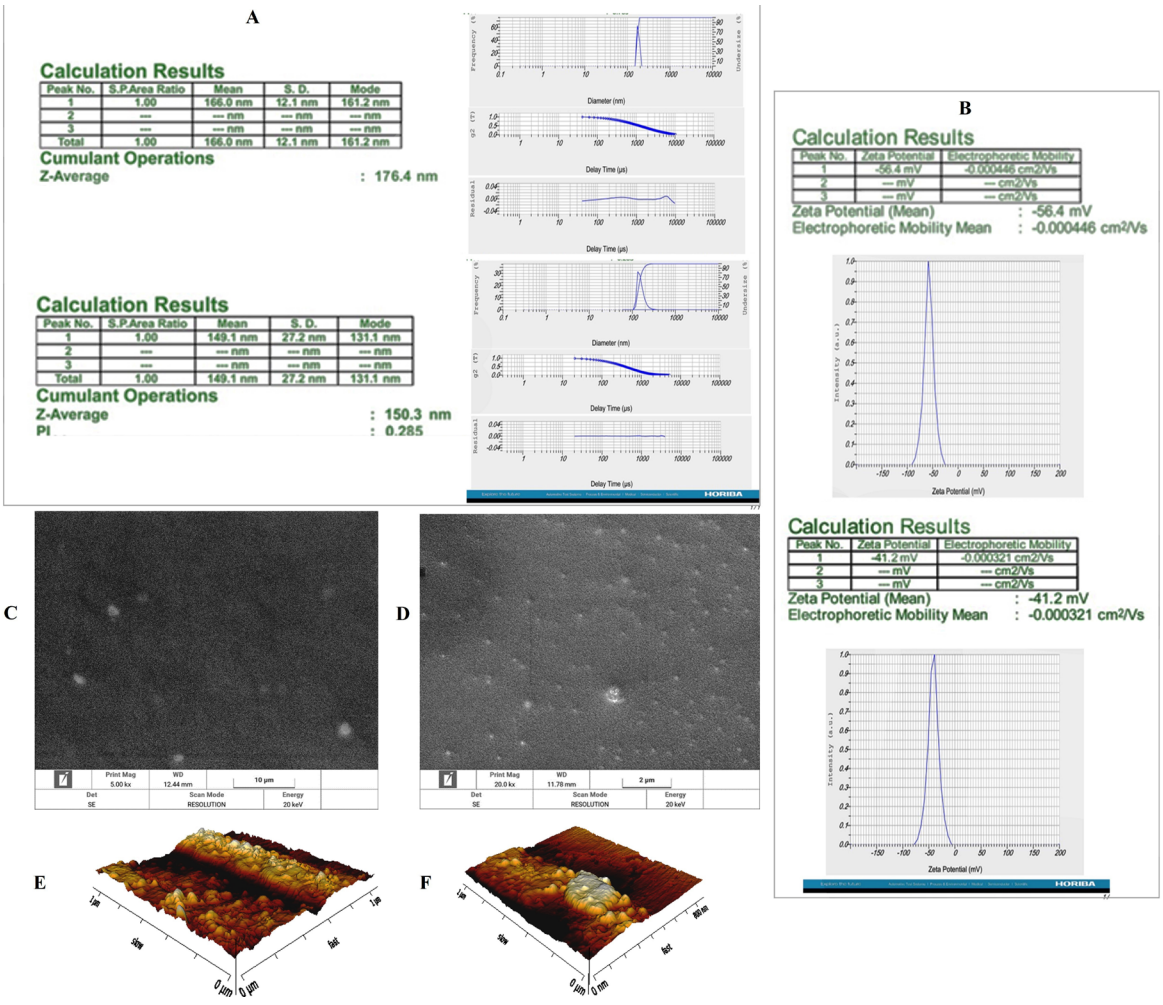


Fig. 1. The particle size and zeta potential; DOX-NPs (A), BBR-NPs (B); Field emission scaninig electron microscopy (FESEM) photography DOX-NPs (C), BBR-NPs(D); Atomic force microscopy photographs DOX-NPs (E), BBR-NPs (F).

BBR release, the calibration chart of drugs in PBS was drawn. According to Fig. 1A, the line equation of DOX and BBR is y= 0.0025 x + 0.0098 and y= 0.001 x - 0.0045, which has a regression coefficient of R2=0.9994 and R2=0.9997, respectively. Based on this graph, the amount of drugs release during 72 hr from nanoparticles was calculated. As shown in Fig. 1B, DOX and BBR were gradually released from PLGA NPs with a biphasic curve, and almost 50% was released at 72 hr. Initial burst of drug release happened at early eight hours that followed slow and contentious release at the second phase. This release behavior was attributed to polymer hydrophobicity, penetration rate of aqueous phase into polymer matrix, drug type and solubility in the nanoparticle. Initial burst of DOX and BBR release was related to the position of the drug on the surface and the simple diffusion process through the matrix of nanoparticles. In contrast, during the second phase, PLGA polymer was cleaved and hydrolyzed by the water solubilization process that results in the drug passage and release steadily through the thicker drug evacuated PLGA layers. This effect has been reported by other research groups [37, 38]. Malinovskayaa et al. demonstrated that the release rate in the first hours is due to drug solubilization and its desorption and in the later phases is related mainly to the both diffusion and PLGA degradation processes [39]. Next the drug release rates were evaluated from DOX and BBR-loaded NP under two pH conditions at 37 °C ad 42 °C. As exhibited in Fig. 2B and C the drug release profiles from the PLGA NPs have thermo and pH-dependent behavior. NPs were fast released ~40 and ~45% of DOX and BBR at pH 5.2 and 42 °C in 8 hr, respectively ($P< 0.05$). The faster DOX and BBR release is related to factors such as the faster degradation of PLGA polymer and the greater DOX solubility at acidic environment [40, 41]. Zhao et al. represented that this phenomenon is mediated by a feeble electrostatic interaction between DOX/BBR and PLGA matrix and also higher hydrolytic destruction of PLGA under acidic pH environment than that at pH 7.4 [42]. Therefore, PLGA nanoparticles are thermo and pH-responsive systems for DOX/BBR delivery and well qualified for the tumors treatment.

### *In vitro cell cytotoxicity assay*

*IC50s for individual DOX and BBR on MCF-7*

Dose–response experiments were performed to investigate the cytotoxicity effect of individual BBR and DOX as a free form and as a PLGA/PVA NPs form on MCF-7. As illustrated in Fig. 3A, individual treatments with the free individual treatment and the NPs forms resulted in the viability inhibition of MCF7 cells in a dose-dependent pattern. The IC50 values of free DOX solution and free BBR solution was 25.14 and 251.1 µg/ml, respectively, and for DOX-loaded PLGA/PVA NPs and BBR-loaded PLGA/

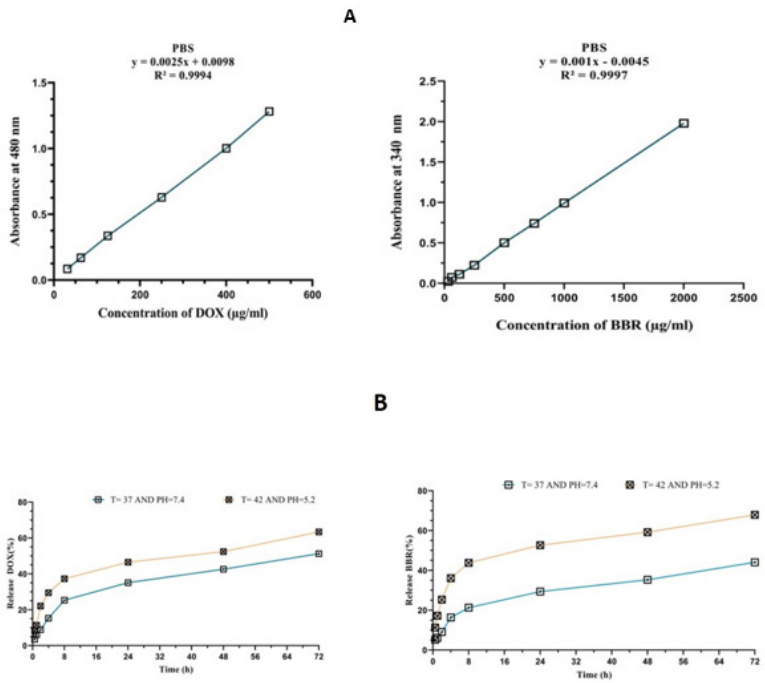

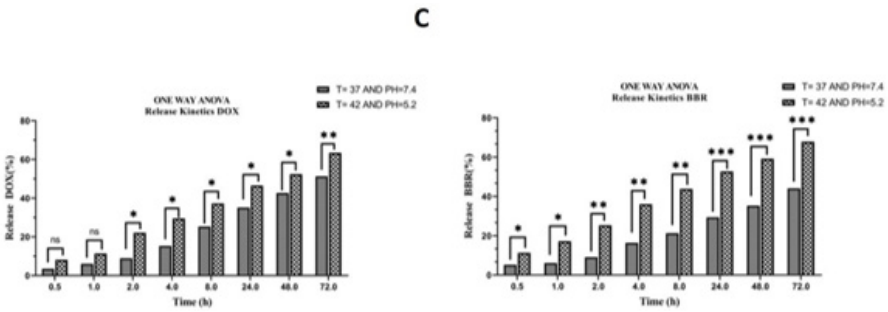


Fig. 2 The drug release profile; (A) Standard curve of DOX and BBR in PBS; (B) In vitro release pattern of DOX and BBR from PLGA NPs in different conditions of temperature and pH; (C) Comparison in DOX and BBR release amount from PLGA NPs at interval times in different temperature and pH. *P-value<0.05, **P-value<0.01 ***P-value<0.001, ns: no significant difference

PVA NPs was 8.28 and 168.9 µg/ml, respectively. To measure the anti- cell proliferative efficacy of blank PLGA/PVA nanoparticles, MTT cell viability assay was accomplished on MCF-10A as a model for normal human mammary epithelial cells and MCF-7 as breast cancer cell. Our results indicated that blank PLGA/PVA NPs had no cytotoxicity (Fig. 3B). This concentration is lower than the maximum amount that we used for treatment. Therefore, at the level used, PLGA/PVA appears to be a safe NP. Our results are consistent with other studies [27, 43-45]. Fig. 3C illustrates that different concentrations of DOX-NPs and BBR-NPs exhibit minimal cytotoxic effects of MCF-10A, the normal breast cells, in comparison to their impact on cancerous cells. This phenomenon can be attributed to the responsiveness of synthesized nanoparticles (NPs) to environmental cues such as temperature and pH. Notably, in normal cell conditions, drug release from these NPs significantly decreases- an essential feature that holds promise for minimizing drug-related side effects on healthy cells [46].

*Comparison of free and NPs form of DOX and BBR*

Given the values of IC50 for 72 hr, revealed that free form of DOX and BBR needed at least a 3.03, and 1.48-fold higher concentration to achieve IC50

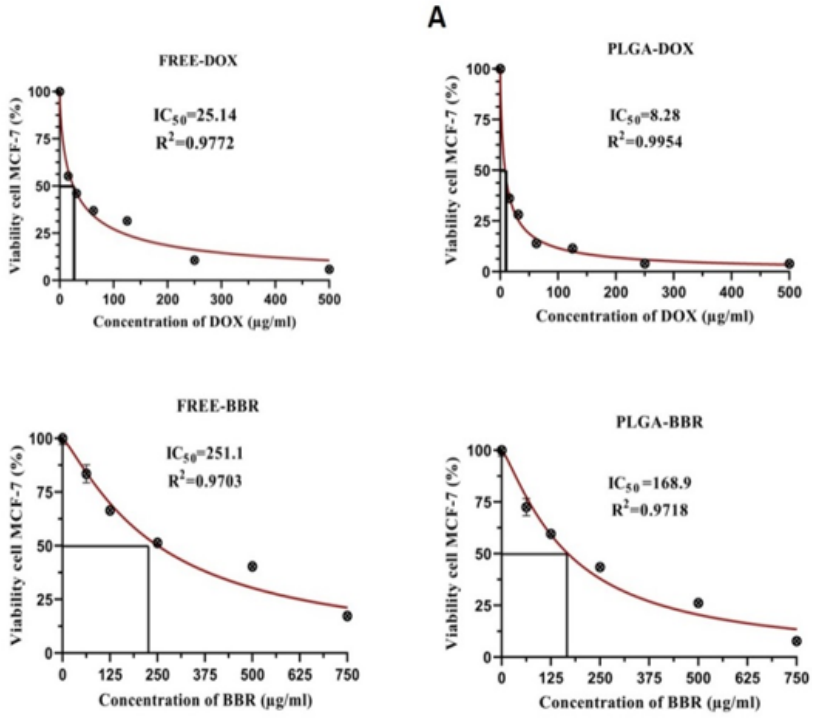

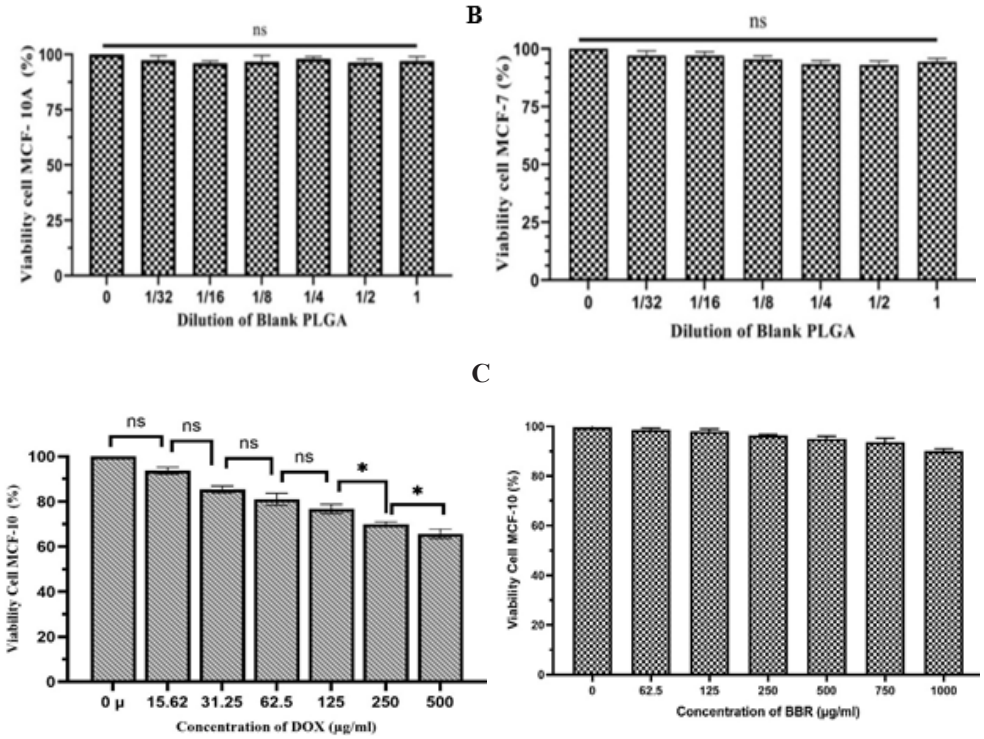


Fig. 3 Inhibition of cell growth by DOX and BBR individual as a drug free form and drug NPs form in MCF-7 cell (A); the cytotoxicity of blank PLGA NPs on MCF-7 and MCF-10A cells after 48 hr (B); the cytotoxicity of various concentration of DOX-NPs and BBR-NPs on MCF-10A as normal cells after 48 hr (C). ns: no significant difference. *: P-value < 0.05

compared to PLGA/PVA form of DOX and BBR, respectively. As depicted in Fig. 4, PLGA/PVA NPs were highly effective in delivering the DOX and BBR drugs to cancer cells. These findings indicated that DOX and BBR in NPs forms had more cytotoxicity compared to that of un-encapsulated forms. Yang et al. developed a Bicalutamideloaded PLGA nanoparticulate (PLGABLT) system to enhance the therapeutic efficacy of BLT in prostate cancer. They showed that nanoparticle-based BLT remarkably improved the therapeutic or anticancer index of the drug. This phenomenon may be related to higher cell internalization and sustained-release pattern of NPs containing drugs [47]. In another work, Shen et al. was designed various formulation of docetaxel (DTX) loaded PLGA nanoparticles to enhance its therapeutic efficiency. It was found that the IC50 of free DTX and DTX-PLGA was 178.2 µg/ml and 28.70 µg/ml, respectively. The viability rate of colon cancer cells was lower in the nanoparticles containing the same concentration of docetaxel [2, 48]. These data are consistent with our results.

*Growth inhibitory effects of DOX- loaded PLGA/PVA NPs in combination with BBR- loaded PLGA/PVA NPs*

The main obstacle in cancer treatment is drug resistance. The combination therapies of chemotherapeutic agents with herbal drugs by targeting several substantial pathways synergistically get over the drug resistance. In this part of study, to determine the synergistic anticancer effects of DOX and BBR, we developed PLGA/PVA NPs that loaded DOX and BBR and compared the cytotoxicity rate of single DOX-PLGA/PVA NPs with combination of DOX-PLGA/PVA NPs and BBR-PLGA/PVA NPs. As shown in Figure 5, the IC50 of DOX/ BBR PLGA/PVA NPs was 5.72 µg/ml compared to single DOX PLGA/PVA NPs 8.28 µg/ml. In fact, IC50 of DOX was diminished to ~1.44 fold in MCF-7 cells. The enhancement of the cancer cells' response to DOX was attained with the combination therapy of BBR which was attributed to the AMPK and HIF-1α downregulation. Studies demonstrated downregulation of AMPK and HIF-1α reverses hypoxia-induced chemoresistance and improves therapeutic index of anticancer agents [49]. Also, BBR is a substrate of P-glycoprotein (P-gp) and downregulates P-gp expression

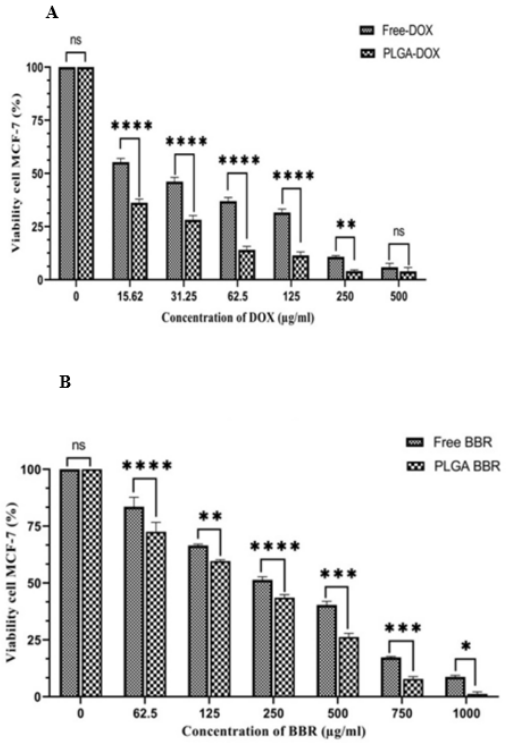


Fig. 4. Comparing cell viability rate of MCF-7 breast cancer cells after treatment with different concentration of A) free DOX, PLGA-DOX, B) free BBR, and PLGA-BBR

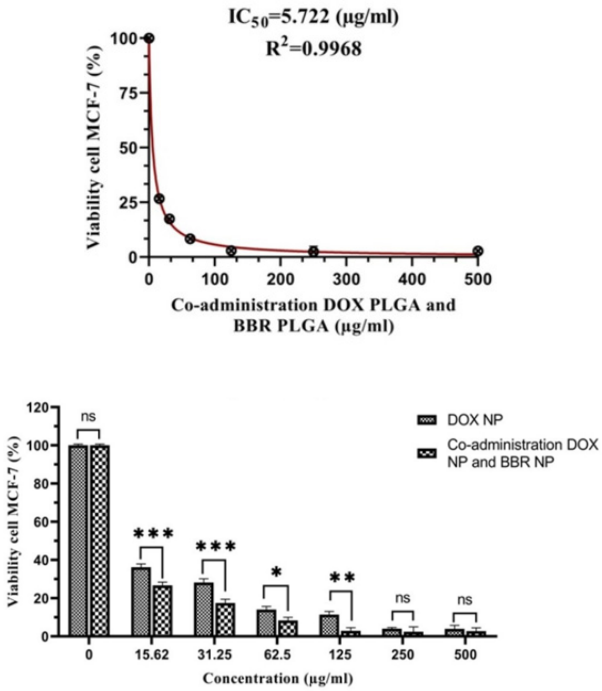


Fig. 5. Analysis of synergy between DOX and BBR for MCF-7; Dose–response curve of DOX PLGA + BBR PLGA (A); Comparison between cytotoxicity of DOX PLGA alone and combined with BBR PLGA at different concentrations

[50]. The increased levels of proinflammatory cytokines and transcription factor NF-κB were decreased by the treatment of BBR [51]. Targeting oncogenic signaling pathways by BBR can be the justification of its synergistic manner with the chemotherapeutic drugs. Tong et al. analyzed the cytotoxicity effect of DOX, BBR and a combination of DOX and BBR on A549, HeLa and HepG2 cells by cell viability experiments in vitro. They revealed that IC50 of combined DOX and BBR was lower than that the drugs which were used alone and the combination of both drugs led to synergistic effects in A549 and HeLa cells and BBR sensitized cells to the anticancer agents of DOX [52]. These findings are consistent with our cytotoxicity experiments. Ruoshi et al. engineered a novel co-delivery strategy to construct a co-loaded liposome of DOX and BBR and the optimal synergistic ratio of the two drugs was monitored using the MTT assay. They found the combination treatment of DOX and BBR significantly suppressed tumor growth in 4T1 murine mammary carcinoma model compared to Doxil, and conquered the DOX-induced myocardial toxicity in mice [3]. Zheng et al. designed self-assembled nanodrug containing BBR and DOX without encapsulation in nanocarrier. They indicated that BBR could remarkably subdue TLR9-MyD88–NF-κB pathway and partly invert DOX- aggravated breast cancer metastasis [53]. BBR not only was known as a chemosensitizer but also have chemoprotector characteristics [17]. It is shown that the application of BBR in combination with DOX may have a potential protective effect against DOX-induced cardiotoxicity [54]. Xiong et al. suggested that BBR protects the heart from DOX toxicity through the involvement of sirtuin 1- (SIRT1-) mediated repression of p66Shc expression. BBR repressed ROS production and mitochondrial damage of cardiac cell by the upregulation of SIRT1 and downregulation of p66shc expression [55]. These findings suggest that BBR can act as chemosensitizer and enhance the cytotoxicity properties of chemotherapeutic agents and also as chemoprotector that preserve normal tissue from toxic agents.

## CONCLUSION

In the present study, we prepared the DOX- and BBR-loaded PLGA/PVA NPs using the double emulsion-solvent evaporation technique. We optimized the formulation through changing the

parameters such as PVA ratio, the molar ratio of polymer/drug and organic phase. Optimum nanoparticle formulations were chosen according to higher encapsulation efficiency and appropriate release rate. The entrapment efficiency (EE) of the ideal nanoparticle formulation for both DOX and BBR exceeded 80%, indicating that the two drugs could be effectively encapsulated in PLGA/PVA NPs. The release data displayed a sustained release of the DOX and BBR with thermosensitive and pH-sensitive manner which can in turn lead to a long-term anticancer efficiency. The viability assay for this optimal formula showed that the IC50s of DOX and BBR loaded on nanoparticles were significantly lower than the free form drugs. The combination strategy of DOX and BBR also indicated a synergistic antitumor effect. The employment of PLGA nanoparticles as a carrier for the concurrent administration of DOX and BBR represents a novel approach to enhance the efficacy of these antineoplastic agents while mitigating the adverse effects associated with the chemotherapeutic medication. This innovative facet of the research warrants further empirical inquiry and validation. Additionally, this novel formulation can be proposed as an adjunctive therapeutic modality for oncology patients after additional and complementary assessment. We concluded that the use of herbal products in combination with antitumor drugs in nanoparticles form can be an appropriate plan to amplify treatment success.

**ACKNOWLEDGMENT**

The author would like to thank NanoBioTechnolodists fardanegar company (NBTF) for their support and collaboration.

**CONFLICT OF INTEREST**

The authors state no conflict of interest.

**FUNDING**

The authors state no funding involved.

**REFERENCES**

1. Hemati M, Haghiralsadat F, Yazdian F, Jafari F, Moradi A, Malekpour-Dehkordi Z. Development and characterization of a novel cationic PEGylated niosome-encapsulated forms of doxorubicin, quercetin and siRNA for the treatment of cancer by using combination therapy. Artif Cells Nanomed Biotechnol. 2019;47(1):1295-1311.
2. Andisheh F, Oroojalian F, Shakour N, Ramezani M, Shamsara J, Khodaverdi E, et al. Docetaxel encapsulation in nanoscale assembly micelles of folate-PEG-docetaxel conjugates for targeted fighting against metastatic breast cancer *in vitro* and *in vivo*. Int J Pharm. 2021;605:120822.
3. Zhang R, Zhang Y, Zhang Y, Wang X, Gao X, Liu Y, et al. Ratiometric delivery of doxorubicin and berberine by liposome enables superior therapeutic index than Doxil ® Asian J Pharm Sci. 2020;15(3):385-396.
4. Yaghoubi F, Motlagh NSH, Naghib SM, Haghiralsadat F, Jaliani HZ, Moradi A. A functionalized graphene oxide with improved cytocompatibility for stimuli-responsive co-delivery of curcumin and doxorubicin in cancer treatment. Sci Rep. 2022;12(1):1959.
5. Oroojalian F, Karimzadeh S, Javanbakht S, Hejazi M, Baradaran B, Webster TJ, et al. Current trends in stimuli-responsive nanotheranostics based on metal–organic frameworks for cancer therapy. Mater Today Energy 2022;57:192-224.
6. Abtahi NA, Naghib SM, Ghalekohneh SJ, Mohammadpour Z, Nazari H, Mosavi SM, et al. Multifunctional stimuli-responsive niosomal nanoparticles for co-delivery and co-administration of gene and bioactive compound: *In vitro* and *in vivo* studies. J Chem Eng. 2022;429:132090.
7. Ghafari M, Haghiralsadat F, Khanamani Falahati-pour S, Zavar Reza J. Development of a novel liposomal nanoparticle formulation of cisplatin to breast cancer therapy. J Cell Biochem. 2020;121(7):3584-3592.
8. Yaghoubi F, Naghib SM, Motlagh NSH, Haghiralsadat F, Jaliani HZ, Tofighi D, et al. Multiresponsive carboxylated graphene oxide-grafted aptamer as a multifunctional nanocarrier for targeted delivery of chemotherapeutics and bioactive compounds in cancer therapy. Nanotechnol Rev. 2021;10(1):1838-1852.
9. Rashidi A, Omidi M, Choolaei M, Nazarzadeh M, Yadegari A, Haghierosadat F, et al. Electromechanical properties of vertically aligned carbon nanotube. Adv Mater Res. 2013;705:332-336.
10. Afereydoon S, Haghiralsadat F, Hamzian N, Shams A, Hemati M, Naghib SM, et al. Multifunctional PEGylated Niosomal Nanoparticle-Loaded Herbal Drugs as a Novel Nano-Radiosensitizer and Stimuli-Sensitive Nanocarrier for Synergistic Cancer Therapy. Front Bioeng Biotechnol. 2022;10:917368.
11. Kim DG, Choi JW, Jo IJ, Kim MJ, Lee HS, Hong SH, et al. Berberine ameliorates lipopolysaccharide-induced inflammatory responses in mouse inner medullary collecting duct-3 cells by downregulation of NF-κB pathway. Mol Med Rep. 2020;21(1):258-266.
12. Li W, Li D, Kuang H, Feng X, Ai W, Wang Y, et al. Berberine increases glucose uptake and intracellular ROS levels by promoting Sirtuin 3 ubiquitination. Biomed Pharmacother. 2020;121:109563.
13. Javed Iqbal M, Quispe C, Javed Z, Sadia H, Qadri QR, Raza S, et al. Nanotechnology-based strategies for berberine delivery system in cancer treatment: pulling strings to keep berberine in power. Front Mol Biosci. 2021;7:624494.
14. Taebpour M, Arasteh F, Akhlaghi M, Haghirosadat BF, Oroojalian F, Tofighi D. Fabrication and characterization of PLGA polymeric nanoparticles containing Berberine and its cytotoxicity on breast cancer cell (MCF-7). Nanomed Res J. 2021;6(4):396-408.
15. Mirrezaei N, Yazdian-Robati R, Oroojalian F, Sahebkar A, Hashemi M. Recent developments in nano-drug delivery systems loaded by phytochemicals for wound healing. Mini-Rev Med Chem. 2020;20(18):1867-1878.
16. Chen Q, Hou Y, Li D, Ding Z, Xu X, Hao B, et al. Berberine induces non-small cell lung cancer apoptosis via the activation of the ROS/ASK1/JNK pathway. Ann Transl Med. 2022;10(8).
17. Devarajan N, Jayaraman S, Mahendra J, Venkatratnam P, Rajagopal P, Palaniappan H, et al. Berberine—A potent

chemosensitizer and chemoprotector to conventional cancer therapies. Phytother Res. 2021;35(6):3059-3077.
18. Oroojalian F, Rezayan AH, Shier WT, Abnous K, Ramezani M. Megalin-targeted enhanced transfection efficiency in cultured human HK-2 renal tubular proximal cells using aminoglycoside-carboxyalkyl-polyethylenimine-containing nanoplexes. Int J Pharm. 2017;523(1):102-120.
19. Fattahi Bafghi A, Haghirosadat BF, Yazdian F, Mirzaei F, Pourmadadi M, Pournasir F, et al. A novel delivery of curcumin by the efficient nanoliposomal approach against Leishmania major. Prep Biochem Biotech. 2021;51(10):990-997.
20. Taebpour M, Akhlaghi M, Shahriary S, Hajihosseini S, Haghiralsadat F, Oroojalian F, et al. Synthesis, physicochemical characterization and pharmaceutical function of niosomal nanoparticles-encapsulated bioactive compound for osteosarcoma treatment. Nanomed J. 2022;9(3):205-215.
21. Ebrahimian M, Mahvelati F, Malaekeh-Nikouei B, Hashemi E, Oroojalian F, Hashemi M. Bromelain loaded lipid-polymer hybrid nanoparticles for oral delivery: Formulation and characterization. Appl Biochem Biotechnol. 2022;194(8):3733-3748.
22. Pieper S, Langer K. Doxorubicin-loaded PLGA nanoparticles-a systematic evaluation of preparation techniques and parameters. Mater Today: Proceedings. 2017;4:S188-S192.
23. Ahmadi F, Bahmyari M, Akbarizadeh A, Alipour S. Doxorubicin-verapamil dual loaded PLGA nanoparticles for overcoming P-glycoprotein mediated resistance in cancer: Effect of verapamil concentration. J Drug Deliv Technol. 2019;53:101206.
24. Khanal S, Adhikari U, Rijal NP, Bhattarai SR, Sankar J, Bhattarai N. pH-responsive PLGA nanoparticle for controlled payload delivery of diclofenac sodium. J Funct Biomater. 2016;7(3):21.
25. Gholami Z, Dadmehr M, Jelodar NB, Hosseini M, Parizi AP. One-pot biosynthesis of CdS quantum dots through *in vitro* regeneration of hairy roots of Rhaphanus sativus L. and their apoptosis effect on MCF-7 and AGS cancerous human cell lines. Materials Research Express. 2020;7(1):015056.
26. Pishavar E, Oroojalian F, Ramezani M, Hashemi M. Cholesterol-conjugated PEGylated PAMAM as an efficient nanocarrier for plasmid encoding interleukin-12 immunogene delivery toward colon cancer cells. Biotechnol Prog. 2020;36(3):e2952.
27. Nia AH, Behnam B, Taghavi S, Oroojalian F, Eshghi H, Shier WT, et al. Evaluation of chemical modification effects on DNA plasmid transfection efficiency of single-walled carbon nanotube–succinate–polyethylenimine conjugates as non-viral gene carriers. MedChemComm. 2017;8(2):364-375.
28. Karimi MA, Dadmehr M, Hosseini M, Korouzhdehi B, Oroojalian F. Sensitive detection of methylated DNA and methyltransferase activity based on the lighting up of FAM-labeled DNA quenched fluorescence by gold nanoparticles. RSC Adv. 2019;9(21):12063-12069.
29. Ghashghaei M, Akhlaghi M. Investigation of nanoniosomal formulation containing doxorubicin effect on ovarian cancer cell line (OVCAR-3 cell line). New cell Mol Biotech J. 2021;11(43):46-62.
30. Ito F, Fujimori H, Honnami H, Kawakami H, Kanamura K, Makino K. Study of types and mixture ratio of organic solvent used to dissolve polymers for preparation of drug-containing PLGA microspheres. Europ Polym J. 2009;45(3):658-667.
31. Alkholief M, Kalam MA, Anwer MK, Alshamsan A. Effect of solvents, stabilizers and the concentration of stabilizers on the physical properties of poly (d, l-lactide-co-glycolide) nanoparticles: Encapsulation, *in vitro* release of indomethacin and cytotoxicity against HepG2-cell. Pharmaceutics. 2022;14(4):870.
32. Danaei M, Dehghankhold M, Ataei S, Hasanzadeh Davarani F, Javanmard R, Dokhani A, et al. Impact of particle size and polydispersity index on the clinical applications of lipidic nanocarrier systems. Pharmaceutics. 2018;10(2):57.
33. Akhlaghi M, Ebrahimpour M, Ansari K, Parnian F, Zarezadeh Mehrizi M, Taebpour M. Synthesis, study and characterization of nano niosomal system containing Glycrrizha glabra extract in order to improve its therapeutic effects. New cell Mol Biotech J. 2021;11(42):65-82.
34. Jeon S, Clavadetscher J, Lee D-K, Chankeshwara SV, Bradley M, Cho W-S. Surface charge-dependent cellular uptake of polystyrene nanoparticles. Nanomaterials. 2018;8(12):1028.
35. Kettler K, Veltman K, van De Meent D, van Wezel A, Hendriks AJ. Cellular uptake of nanoparticles as determined by particle properties, experimental conditions, and cell type. Environ Toxicol Chem. 2014;33(3):481-492.
36. Zhang D, Wei L, Zhong M, Xiao L, Li H-W, Wang J. The morphology and surface charge-dependent cellular uptake efficiency of upconversion nanostructures revealed by single-particle optical microscopy. Chem Sci. 2018;9(23):5260-5269.
37. Alamdari SG, Alibakhshi A, de la Guardia M, Baradaran B, Mohammadzadeh R, Amini M, Kesharwani P, Mokhtarzadeh A, Oroojalian F, Sahebkar A. Conductive and semiconductive nanocomposite-based hydrogels for cardiac tissue engineering. Adv Healthc Mater. 2022;11(18):2200526.
38. Yoo J, Won Y-Y. Phenomenology of the initial burst release of drugs from PLGA microparticles. ACS Biomater Sci Eng. 2020;6(11):6053-6062.
39. Malinovskaya Y, Melnikov P, Baklaushev V, Gabashvili A, Osipova N, Mantrov S, et al. Delivery of doxorubicin-loaded PLGA nanoparticles into U87 human glioblastoma cells. Int J Pharm. 2017;524(1-2):77-90.
40. Scheeren LE, Nogueira-Librelotto DR, Macedo LB, de Vargas JM, Mitjans M, Vinardell MP, et al. Transferrin-conjugated doxorubicin-loaded PLGA nanoparticles with pH-responsive behavior: a synergistic approach for cancer therapy. J Nanoparticle Res. 2020;22:1-18.
41. Montha W, Maneeprakorn W, Buatong N, Tang I-M, Pon-On W. Synthesis of doxorubicin-PLGA loaded chitosan stabilized (Mn, Zn) Fe2O4 nanoparticles: biological activity and pH-responsive drug release. Mater Sci Eng C. 2016;59:235-240.
42. Zhao J, Yang H, Li J, Wang Y, Wang X. Fabrication of pH-responsive PLGA (UCNPs/DOX) nanocapsules with upconversion luminescence for drug delivery. Sci Rep. 2017;7(1):1-11.
43. Ibrahim WN, Muizzuddin Bin Mohd Rosli L, Doolaanea AA. Formulation, cellular uptake and cytotoxicity of thymoquinone-loaded plga nanoparticles in malignant melanoma cancer cells. Int J Nanomedicine. 2020:8059-8074.
44. Watcharadulyarat N, Rattanatayarom M, Ruangsawasdi N, Patikarnmonthon N. PEG–PLGA nanoparticles for encapsulating ciprofloxacin. Sci Rep. 2023;13(1):266.
45. Pourpirali R, Mahmoudnezhad A, Oroojalian F, Zarghami N, Pilehvar Y. Prolonged proliferation and delayed senescence of the adipose-derived stem cells grown on the electrospun composite nanofiber co-encapsulated with TiO2 nanoparticles and metformin-loaded mesoporous silica nanoparticles. Int J Pharm. 2021;604:120733.

46. Akbari P, Taebpour M, Akhlaghi M, Hasan SH, Shahriyari S, Parsaeian M, et al. Regulation of the P53 tumor suppressor gene and the Mcl-2 oncogene expression by an active herbal component delivered through a smart thermo-pH-sensitive PLGA carrier to improve Osteosarcoma treatment. Med Oncol. 2024;41(3):68.
47. Guo J, Wu SH, Ren WG, Wang XL, Yang AQ. Anticancer activity of bicalutamide-loaded PLGA nanoparticles in prostate cancers. Exp Ther Med. 2015;10(6):2305-2310.
48. Yang Y, Yin Y, Zhang J, Zuo T, Liang X, Li J, et al. Folate and borneol modified bifunctional nanoparticles for enhanced oral absorption. Pharmaceutics. 2018;10(3):146.
49. Pan Y, Shao D, Zhao Y, Zhang F, Zheng X, Tan Y, et al. Berberine reverses hypoxia-induced chemoresistance in breast cancer through the inhibition of AMPK-HIF-1α. Int J Biol Sci. 2017;13(6):794.
50. Zhang Y, Guo L, Huang J, Sun Y, He F, Zloh M, et al. Inhibitory effect of berberine on broiler P-glycoprotein expression and function: *in situ* and *in vitro* studies. Int J Mol Sci. 2019;20(8):1966.
51. Almatroodi SA, Alsahli MA, Rahmani AH. Berberine: An important emphasis on its anticancer effects through modulation of various cell signaling pathways. Molecules. 2022;27(18):5889.
52. Tong N, Zhang J, Chen Y, Li Z, Luo Y, Zuo H, et al. Berberine sensitizes mutliple human cancer cells to the anticancer effects of doxorubicin *in vitro*. Oncol Lett. 2012;3(6):1263-1267.
53. Zheng X, Zhao Y, Jia Y, Shao D, Zhang F, Sun M, et al. Biomimetic co-assembled nanodrug of doxorubicin and berberine suppresses chemotherapy-exacerbated breast cancer metastasis. Biomaterials. 2021;271:120716.
54. Chen X, Zhang Y, Zhu Z, Liu H, Guo H, Xiong C, et al. Protective effect of berberine on doxorubicin-induced acute hepatorenal toxicity in rats. Mol Med Rep. 2016;13(5):3953-3960.
55. Wu Y-Z, Zhang L, Wu Z-X, Shan T-t, Xiong C. Berberine ameliorates doxorubicin-induced cardiotoxicity via a SIRT1/p66Shc-mediated pathway. Oxid Med Cell Longev. 2019:2019:2150394.